

Received February 24, 2021, accepted March 14, 2021, date of publication March 18, 2021, date of current version March 29, 2021.

Digital Object Identifier 10.1109/ACCESS.2021.3067064

Polarization-Reconfigurable Antenna Using Combination of Circular Polarized Modes

SHENYUN WANG^{1,2}, (Member, IEEE), DANPING YANG², WEN GEYI^{1,2}, (Fellow, IEEE), CHEN ZHAO², (Member, IEEE), AND GUOWEN DING^{1,2}, (Member, IEEE)

¹School of Electronic and Information Engineering, Nanjing University of Information Science and Technology, Nanjing 210044, China

²Research Center of Applied Electromagnetics, Nanjing University of Information Science and Technology, Nanjing 210044, China

Corresponding author: Guowen Ding (gwding@nuist.edu.cn)

This work was supported in part by the National Natural Science Foundation of China under Grant 61971231, in part by the Chongqing Key Laboratory of Mobile Communications Technology under Grant cqupt-mct-201803, and in part by the Startup Foundation for Introducing Talent of the Nanjing University of Information Science and Technology (NUIST).

ABSTRACT This paper presents a novel polarization-reconfigurable antenna based on the combination of circularly polarized (CP) modes, which is capable of changing its polarization states among arbitrary linear polarizations (LPs), left-handed circular polarization (LHCP) and right-handed circular polarization (RHCP). A truncated square patch with two isolated aperture-coupling feeds is used as radiation element operating at 2.45 GHz, which can operate in two orthogonal CP modes with low crosstalk. By exciting one of the two feeding microstrip lines, LHCP or RHCP mode can be independently generated. Meanwhile, by simultaneously exciting the two feeding microstrip lines with identical amplitudes but with different initial phases, LP mode with polarization plane oriented in any desired azimuth direction can be obtained. The simulated and measured peak gain of the proposed antenna remains at about 6.8 dBi at 2.45 GHz and the impedance matching bandwidth ranging from 2.25 to 2.60 GHz is fully overlapped for all the polarization states. Experimental results show a good performance of the proposed antenna.

INDEX TERMS Polarization reconfigurable antenna, continuous linear polarization, circular polarization, mode combination.


I. INTRODUCTION

Polarization-reconfigurable antennas, which can switch their polarization states, are commonly engineered where polarization diversity is needed, such as wireless communication systems, radars and navigations. In wireless communication systems (mobile satellite communications, GNSS, WLAN, RFID, etc.), polarization-reconfigurable antennas are desired to mitigate multipath fading losses and/or to improve the signal transmission performance by avoiding the polarization mismatch and interference with the other systems [1]–[4]. In imaging radars, components to control the polarization state of detecting wave are critical to describe the target characteristics [5].

Several schemes have been proposed to switch the polarization states of an antenna (or antenna array), where electrical control components such as PIN diodes or RF-MEMS are usually employed [6]–[20]. An antenna can be switched

between various polarization states by using reconfigurable feeding network to feed different parts of the antenna [6]–[15]. Meanwhile, electrical control components can also be directly used to introduce perturbation segments on the radiating part of the antenna, thus leading to different polarization states [16]–[24]. Recently, a new scheme was proposed by using an electronically reconfigurable polarizer integrated with a linearly polarized (LP) antenna [25], [26], which has an advantage of complete isolation of the DC bias from the RF signal and a gain improvement.

For a device-to-device communication system, the polarization mismatch caused by the environmental changes may degrade the power efficiency and the communication link capacity. To reduce the polarization mismatch and receive an arbitrarily polarized wave, traditional solution is to adopt a circularly polarized (CP) antenna as the receiving antenna. Although a CP antenna can receive a LP wave polarized in arbitrary azimuth direction, it only has a maximum efficiency of 50%. Moreover, when a CP antenna receives a CP wave with opposite rotation, the polarization efficiency

The associate editor coordinating the review of this manuscript and approving it for publication was Debabrata Karmakar .

is extremely low. To resolve this issue, polarization reconfigurable antennas can be used as a good candidate. At present, most proposed polarization reconfigurable antennas are designed to change either the polarization plane of LP waves, the handedness of the CP wave or both LP and CP states. However, the polarization states reported in the above-mentioned literatures are usually discrete and limited. To improve the polarization efficiency for receiving LP waves, multi-linear polarization reconfigurable antennas have been reported [27], [28]. For instance, a linear polarization reconfigurable antenna with Quad-polarization diversity is proposed, whose polarization mismatch is reduced to less than -0.69dB . Furthermore, the polarization mismatch will be perfectly mitigated when the LP reconfigurable antenna can continuously change its polarization plane. Recently, liquid metal alloy is employed to tune the angle of LP wave continuously by changing the symmetry axis of the antenna structure [29], [30], but its slow tuning speed and the large pump equipment hinder the application of the liquid metal tuning technique. The polarization plane of a LP wave can be continuously controlled by combining two orthogonal LP modes [31] or two orthogonal CP modes [32], where a tunable power divider or phase shifter are employed. However, the azimuth tuning ranges of the LP plane are limited due to the structures and working principles. In addition, the overlapped impedance bandwidth of most reported antennas is less than 10% when their polarization states being switched among the LP modes and CP modes. It is mainly due to the fact that CP modes are usually generated by two degenerate orthogonal linear modes with equal amplitude, while the LP modes are independently generated [13], [33].

In this paper, a dual-circularly polarized patch antenna fed by two isolated apertures is employed as the radiating element. When one of the two apertures is excited through coupling the electromagnetic energy from the feeding microstrip line, right-handed circularly polarized (RHCP) wave or left-handed circularly polarized (LHCP) wave can be generated. While the two apertures are simultaneously fed with identical amplitudes and certain initial phase difference, LP wave with polarization plane in arbitrary azimuth direction is radiated by the combination of the two orthogonal CP components. The proposed scheme makes the impedance bandwidth fully overlapped among the CP modes and continuous LP modes. The topological structure and working principle of the antenna are presented in Section II. The reconfigurable polarization states switching among CP modes and continuous LP modes are validated in Section III. In Section IV, the conclusions are drawn.

II. ANTENNA DESIGN

A. ANTENNA CONFIGURATION

The topological structure of the proposed dual-circularly polarized patch antenna is shown in Fig.1. It consists of two square substrate layers, where a truncated square metal patch is printed on the top side of the top substrate, as show

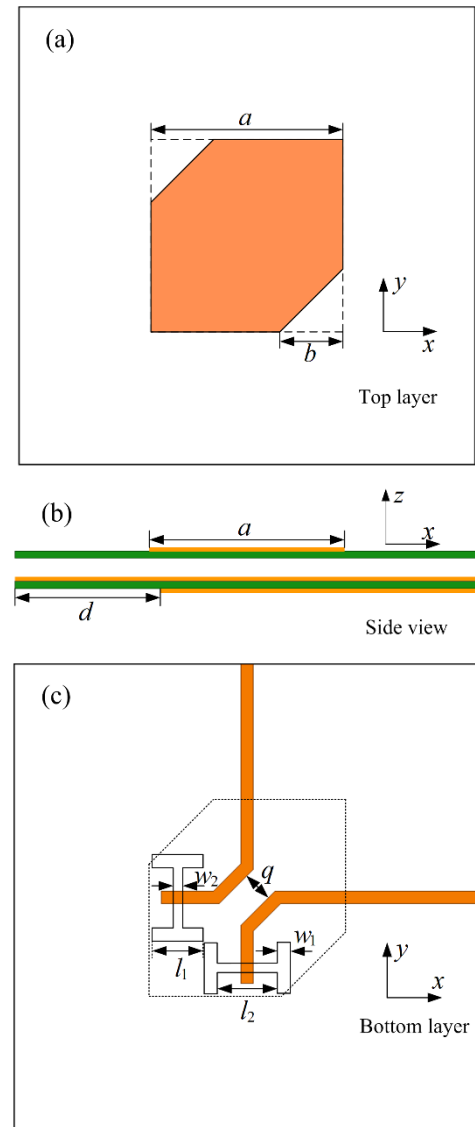


FIGURE 1. Configuration of the dual-circularly polarized patch element: (a) top layer, (b) side view, and (c) bottom layer.

in Fig.1 (a). The two square substrates are FR4 with relative permittivity of 4.7 and loss tangent of 0.02. The thickness and side-length of the substrate are 1.5 mm and 100 mm, respectively. The top substrate is mounted over the ground plane with a height of 8.0 mm to broaden its operating frequency band, as shown in Fig.1 (b). Two orthogonally oriented H-shaped apertures are etched on the ground plane that is etched on the top side of the bottom substrate to excite two orthogonal CP modes. Two feeding microstrip lines with characteristic impedance of 50 Ohm are designed on the opposite side of the bottom substrate to couple the feeding electromagnetic energy to radiation element through the corresponding aperture, as shown in Fig.1 (c).

The proposed polarization reconfigurable patch antenna is designed to operate at 2.45 GHz and the geometrical parameters of the patch structure denoted in Fig.1 are optimized

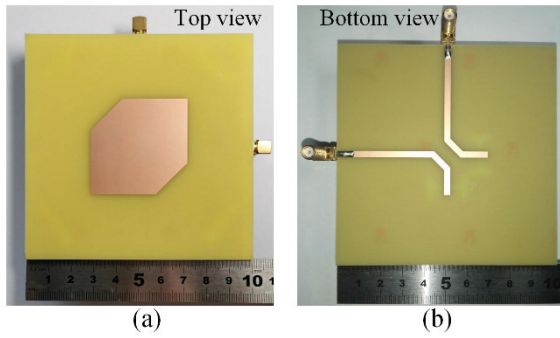


FIGURE 2. Photo of the reconfigurable antenna: (a) top view, and (b) bottom view.

to be: $a = 42.2$ mm, $b = 13.8$ mm, $l_1 = 3.0$ mm, $w_1 = 2.0$ mm, $l_2 = 11.0$ mm, $w_2 = 2.8$ mm, $q = 6.5$ mm. The proposed antenna is designed and optimized using a commercial full-wave simulator, ANSYS High Frequency Structural Simulator (HFSS). To verify the proposed design scheme, a prototype is fabricated to validate the polarization reconfigurable capabilities. The top and bottom pictures are shown in Figs.2 (a) and (b), respectively, where the top substrate is supported by four foam cylinders and the feeding microstrip lines are excited by using SMA connectors to connect with a tunable feeding circuit.

B. RECONFIGURABLE PRINCIPLE

An arbitrary LP wave can be decomposed into two orthogonal CP components. Therefore, a way to realize an arbitrary LP wave is to excite two suitable orthogonal CP waves simultaneously. The proposed patch element can independently operate in LHCP or RHCP modes (namely dual-circularly polarized modes) by exciting one of the feeding microstrip lines. As shown in Fig.1 (c), when the vertical microstrip line is excited, the antenna radiates an LHCP wave in the main radiation direction and the E-field can be expressed as:

$$\mathbf{E}_{\text{LHCP}} = \hat{\mathbf{x}}E_0e^{j(\omega t - kz - \frac{\pi}{2})} + \hat{\mathbf{y}}E_0e^{j(\omega t - kz + 0)} \quad (1)$$

where E_0 stands for the amplitude of the radiation and it is regarded to be a real number. Similarly, when the horizontal microstrip line is excited, the antenna radiates an RHCP wave in the main radiation direction and the corresponding E-field can be expressed as:

$$\mathbf{E}_{\text{RHCP}} = \hat{\mathbf{x}}E_0e^{j(\omega t - kz + 0)} + \hat{\mathbf{y}}E_0e^{j(\omega t - kz - \frac{\pi}{2})} \quad (2)$$

When the two microstrip lines are excited simultaneously, the radiation amplitude of each CP wave is normalized to be $E_0/\sqrt{2}$ and the radiated wave is given by:

$$\begin{aligned} \mathbf{E}_{\text{LP}} &= \frac{1}{\sqrt{2}}\mathbf{E}_{\text{LHCP}} + \frac{1}{\sqrt{2}}\mathbf{E}_{\text{RHCP}} \\ &= \hat{\mathbf{x}}E_0e^{j(\omega t - kz - \frac{\pi}{4})} + \hat{\mathbf{y}}E_0e^{j(\omega t - kz - \frac{\pi}{4})} \end{aligned} \quad (3)$$

It is obvious that an LP wave can be generated by the combination of LHCP and RHCP components, where the x - and y -components have identical amplitudes and are

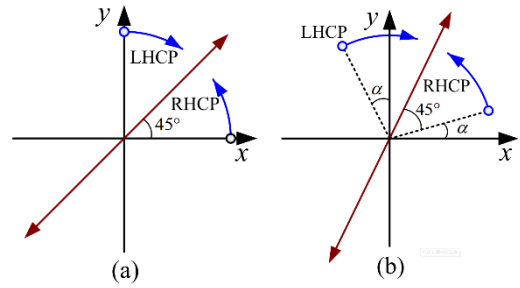


FIGURE 3. Schematic of LP wave generated by combination of LHCP and RHCP waves: (a) $\alpha = 0^\circ$, and (b) $\alpha \neq 0^\circ$.

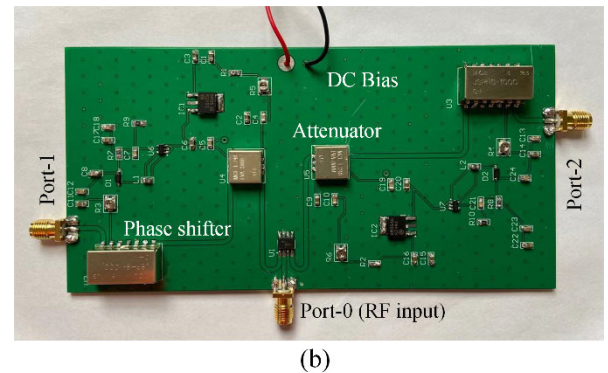
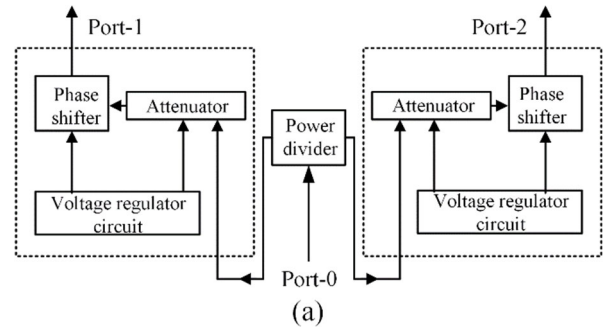


FIGURE 4. The design of the feeding circuit. (a) Schematic. (b) Photo.

in phase. As shown in Fig.3 (a), the generated LP wave given in Eq. (3) has a polarization plane at azimuth of $\pi/4$ (or 45°), as illustrated in Fig.3(a). Next, we make the initial phase of the LHCP mode excitation delayed by α and that of the RHCP mode excitation advanced by α . In this case, the excited LHCP and RHCP waves can be rewritten as:

$$\mathbf{E}'_{\text{LHCP}} = \mathbf{E}_{\text{LHCP}} \cdot e^{j(-\alpha)} \quad (4)$$

$$\mathbf{E}'_{\text{RHCP}} = \mathbf{E}_{\text{RHCP}} \cdot e^{j(+\alpha)} \quad (5)$$

The generated LHCP and RHCP waves illustrated in Eq. (4) and Eq. (5) are combined into a LP wave whose polarization plane is oriented at azimuth of $\pi/4 + \alpha$. When the initial phases $\pm\alpha$ of the two feeding microstrip lines are changed by tuning the continuous phase shifters on the feeding circuit, the polarization plane of the LP wave can be continuously changed, as illustrated in Fig.3(b). In contrast to the reports in [29] and [30], the azimuth of the polarization

TABLE 1. Channel attenuation of the feeding circuit.

States (phase shift)	Attenuation ($ S10 ^2, S20 ^2$)	Radiation efficiency	Antenna efficiency
RHCP($\alpha=0^\circ$)	0.32dB, 35.0dB	77.65%	37.58%
LHCP($\alpha=0^\circ$)	35.0dB, 0.32dB	77.69%	37.60%
45°LP($\alpha=0^\circ$)	0.32dB, 0.32dB	76.64%	74.19%
60°LP($\alpha=15^\circ$)	0.35dB, 0.35dB	76.78%	74.09%
30°LP($\alpha=-15^\circ$)	0.35dB, 0.35dB	76.77%	74.08%
90°LP($\alpha=45^\circ$)	0.38dB, 0.38dB	77.67%	74.80%
0°LP($\alpha=-45^\circ$)	0.38dB, 0.38dB	77.66%	74.79%
120°LP($\alpha=75^\circ$)	0.46dB, 0.46dB	78.56%	75.02%
135°LP($\alpha=90^\circ$)	0.56dB, 0.56dB	78.69%	74.36%
150°LP($\alpha=105^\circ$)	0.64dB, 0.64dB	78.55%	73.68%

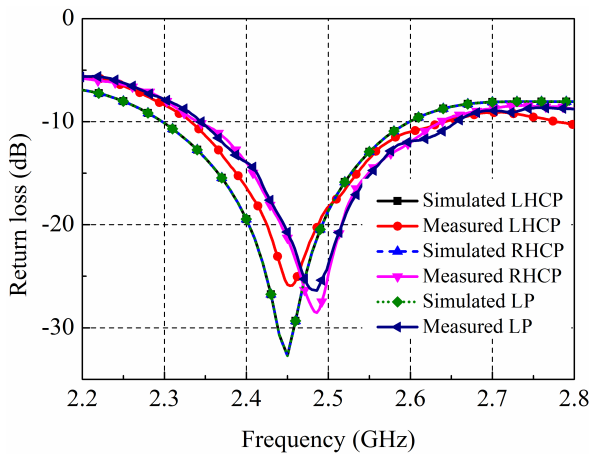


FIGURE 5. Measured and simulated reflection coefficients (S11) of the fabricated antenna.

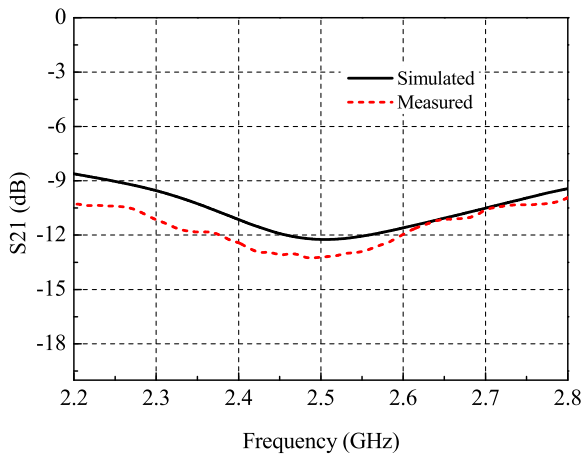


FIGURE 6. Measured and simulated isolation of the two feeding microstrip lines.

plane of the LP wave presented in this paper can be continuously tuned in an azimuth range of 360°. Finally, multi-polarization states (LHCP, RHCP and continuous LP modes) can also be generated based on the proposed reconfigurable principle.

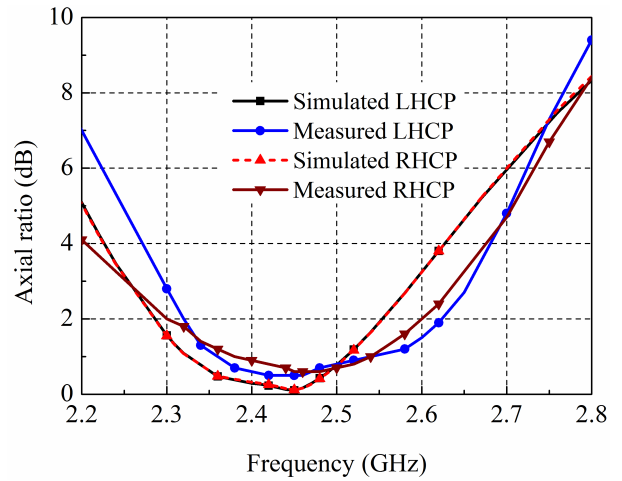


FIGURE 7. Measured and simulated axial ratio of the antenna working in two CP modes.

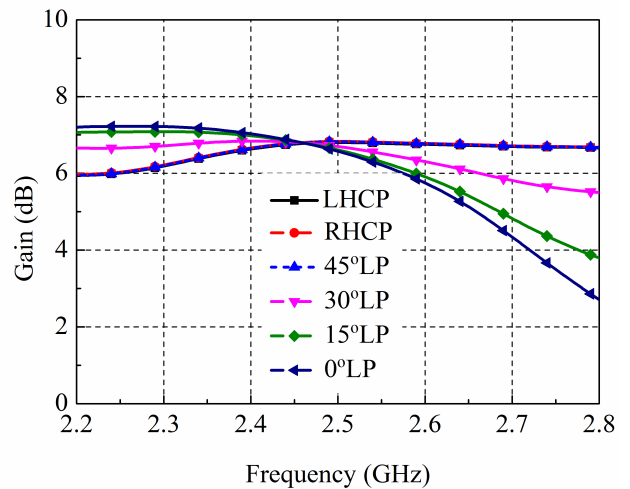


FIGURE 8. Simulated gain of the antenna working in various polarization states.

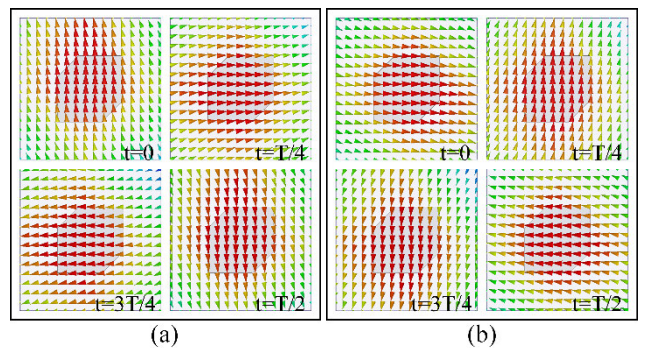


FIGURE 9. Electrical field vector distributions on the radiation aperture at different time when the antenna works in (a) LHCP mode and (b) RHCP mode.

C. FEEDING NETWORK

To avoid using large number of RF switches, a general feeding circuit is designed to feed the two microstrip lines,

as shown in Fig.4. A T-type microstrip power divider is utilized to divide the signal injected from port-0 into two channels, which terminate at port-1 and port-2. In each signal channel, a bias voltage controllable phase shifter and attenuator are employed to regulate the output phase and amplitude, as shown in Fig.4 (a). Microstrip transmission lines with characteristic impedance of 50Ω are used to connect the lumped phase shifters and attenuators and to ensure impedance matching. The photo of the voltage-controlled feeding circuit is shown in Fig.4 (b). When one attenuator is set with a large attenuation ($>35\text{dB}$) and the other is set with near no attenuation by adjusting the control voltage, one RF output channel is suppressed and the other is switched on. In this case, a CP mode (LHCP or RHCP mode) is solely excited. By independently adjusting the rheostat on the voltage regulator circuit to control the phase shifter on the two channels, the desired initial phase (corresponding to the parameter $\pm\alpha$) fed to the two antenna ports are achieved for the continuous tuning of the polarization plane of LP mode. In this case, the two attenuators are simultaneously set with very low attenuation. Such a feeding circuit provide a convenient way to tuning the amplitudes and phases fed to the two ports of the patch. The attenuation on each channel caused by the introduction of attenuator and phase shifters will reduce the total antenna efficiency (AE), which is determined by both the radiation efficiency (RE) of the radiation patch and the attenuation of the feeding circuit. The RE and AE are defined by:

$$RE = P_{\text{rad}} / (P_{\text{in1}} + P_{\text{in2}}) \quad (6)$$

$$AE = P_{\text{rad}} / P_{\text{in0}} \quad (7)$$

where P_{rad} is the radiated power, P_{in1} and P_{in2} are the input power for the radiation patch through the two feeding microstrip lines and P_{in0} is the total input power injected into the feeding circuit. The channel attenuation in the feeding circuit mainly attributes to the insertion loss of the phase shifter, the attenuation of the attenuator, the loss on transmission lines and the return loss. The tested channel attenuation of feeding circuit for exciting CP modes and LP modes with different shift phase α at $0, \pm 15^\circ, \pm 45^\circ, 75^\circ, 90^\circ$ and 105° are recorded in Table 1.

III. RESULTS AND DISCUSSIONS

According to the design principle, if only one of the feeding microstrip lines is excited, an LHCP wave or an RHCP one will be generated by the truncated square patch. When the two feeding microstrip lines are simultaneously excited with an initial phase difference, an LP wave will be obtained with its polarization plane oriented in a desired azimuth direction.

To validate the above presented theory, the simulated and measured reflection coefficients of the antenna with different polarization states are given in Fig.5. It can be seen that the simulated matched impedance bandwidth ($S_{11} \leq -10\text{dB}$) ranging from 2.34 to 2.66GHz is fully overlapped for all the polarization states. The feeding lines and radiating patch of

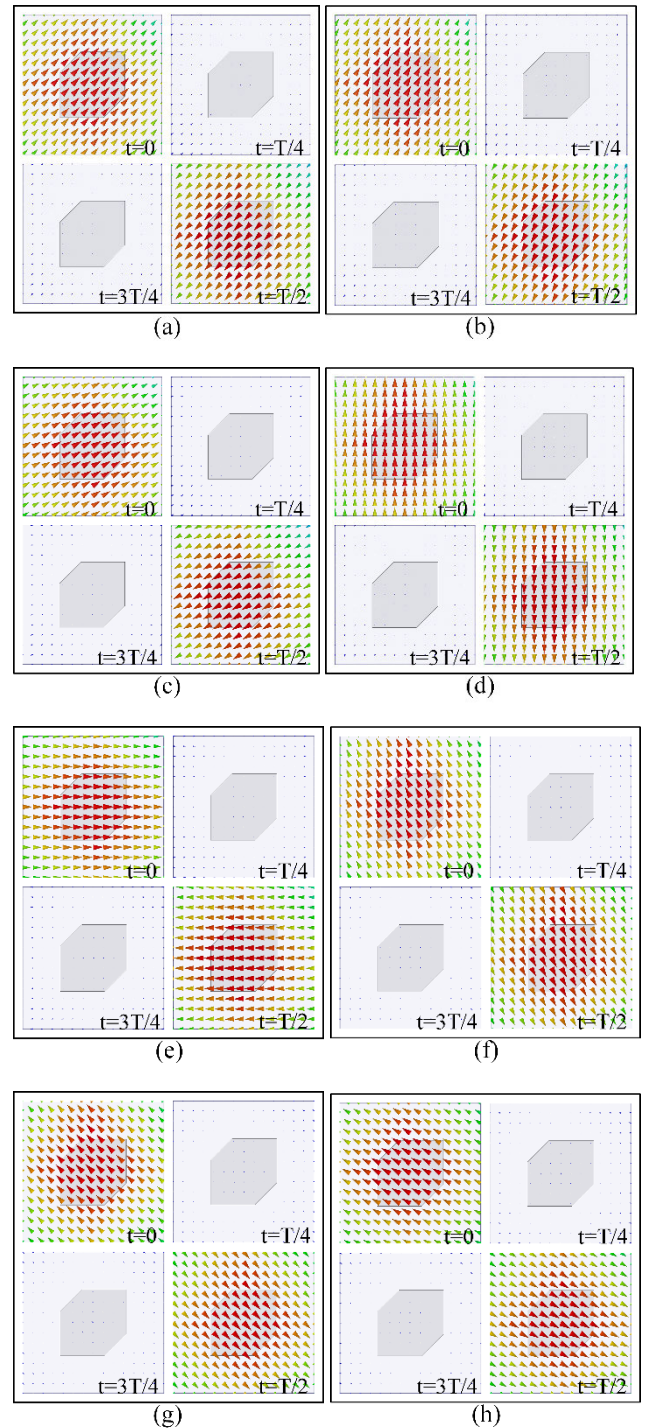


FIGURE 10. Electrical field vector distributions on the radiation aperture at different time when the antenna works in LP modes with the polarization plane at azimuth of (a) 45° , (b) 60° , (c) 30° , (d) 90° , (e) 0° , (f) 120° , (g) 135° and (h) 150° .

the antenna is symmetric along the axis of azimuth at 45° and the simulated and measured transmission coefficients (S_{21} and S_{12}) of the two feeding ports are less than -12.1dB and -13.0dB , respectively, as shown in Fig.6. The signal coupling between the two ports may reduce the RE and

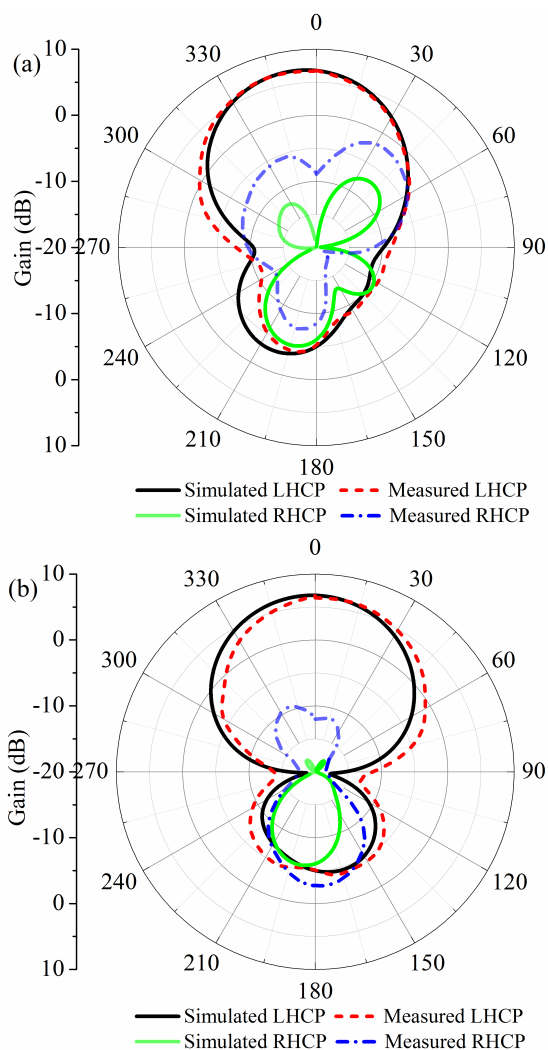


FIGURE 11. Gain patterns of the LHCP mode on the (a) xz-plane and (b) yz-plane.

AE to some extent. Considering the isolation of the two antenna feeding ports and channel attenuation of the feeding circuit, RE and AE of the proposed antenna are calculated and recorded in Table 1. For CP modes, the antenna efficiency is badly reduced (<50%) due to the suppression of one channel. For LP modes, two channels are simultaneously switched on with very low attenuation of the two attenuators, thus leading to higher antenna efficiencies (>73%). According to the definition of the RE, there is no significant RE difference among all the polarization states. Low AE for the CP modes attributes to the large attenuation of one channel on the feeding circuit. Moreover, the realized two orthogonal CP modes have same matched impedance bandwidth, as well as the axial ratio (AR) bandwidth, as shown in Fig.7. The simulated 3.0 dB AR bandwidth of the CP modes ranges from 2.29 to 2.60 GHz. Moreover, the realized two orthogonal CP modes have same matched impedance bandwidth, as well as the axial ratio (AR) bandwidth, as shown in Fig.7. The simulated 3.0 dB AR bandwidth of the CP modes ranges from 2.29 to 2.60 GHz.

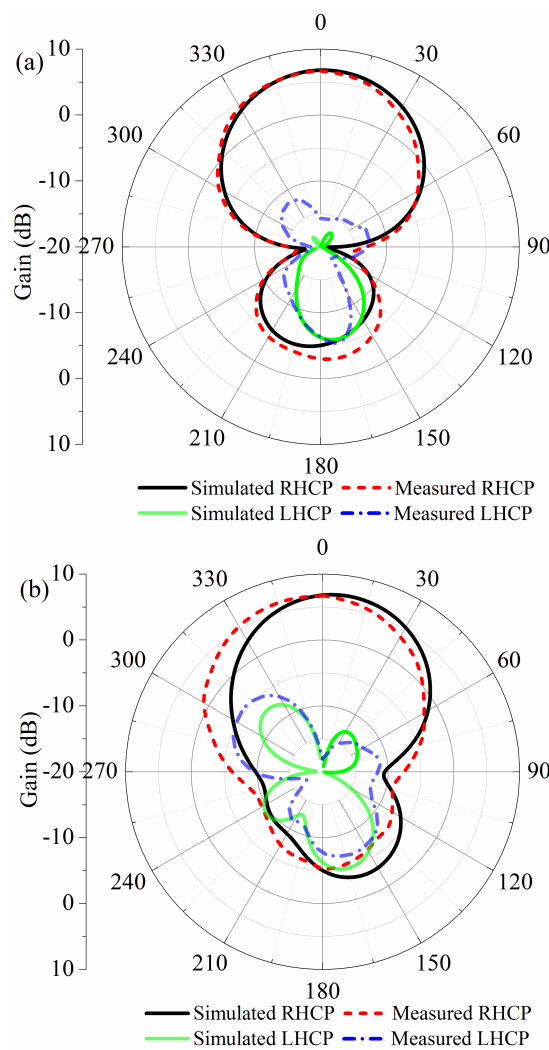


FIGURE 12. Gain patterns of the RHCP mode on the (a) xz-plane and (b) yz-plane.

The peak gain of the antenna in the main radiation direction is simulated when it operates in CP modes and LP modes in different azimuth directions, as shown in Fig.8. It can be found that the peak gain ranges from 6.2 to 6.8 dBi across the impedance matching bandwidth (2.34-2.66 GHz) when it works in CP modes and 45° LP mode. By adjusting the initial phase, the polarization plane of the LP mode can be turned from 45° to 0°, and the resultant gain fluctuation versus frequency is expanded. For 0° LP mode, the gain monotonously decreases from 7.2 dBi to 5.7 dBi with the frequency varying from 2.29 to 2.60 GHz. It should be pointed out that the gain remains stable at 6.8 dBi at 2.45GHz for all the polarization states, as shown in Fig.8.

To better demonstrate the performance of the proposed antenna at various polarization states, the surface electrical field distributions on a radiation plane at distance of 8.0 cm away from radiation patch are simulated. When the vertical feeding microstrip line is excited, the antenna operates

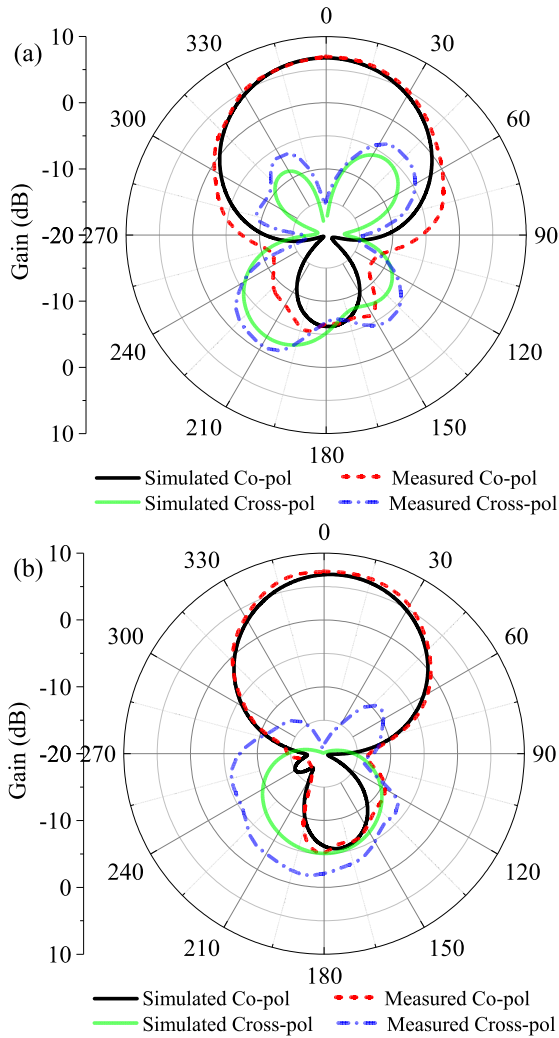


FIGURE 13. Gain patterns of LP mode at 0 azimuth on the (a) co-polar plane and (b) cross-polar plane.

in LHCP mode, and the surface electrical field distributions at different time in one sinusoidal period are plotted in Fig.9 (a). When the horizontal feeding microstrip line is excited, the antenna operates in RHCP mode, and the surface electrical field distributions at different time in one sinusoidal period are plotted in Fig.9 (b). It is obvious that the electrical field vector rotates clockwise or anticlockwise with time increase, while the amplitude is almost kept unchanged, which stands for an LHCP or RHCP wave radiation.

Next, when the two feeding microstrip lines are excited simultaneously through the feeding circuit with identical amplitudes and different initial phases, an LP wave can be combined. Supposing that the initial phase of the excitation for LHCP mode is delayed by α , while the phase of the excitation for RHCP mode is initially advanced by α , the combined LP wave has a linear polarization plane in azimuth direction at $45^\circ + \alpha$. Specially, the phase parameter α is set to be $0^\circ, \pm 15^\circ, \pm 45^\circ, 75^\circ, 90^\circ$ and 105° , the resultant

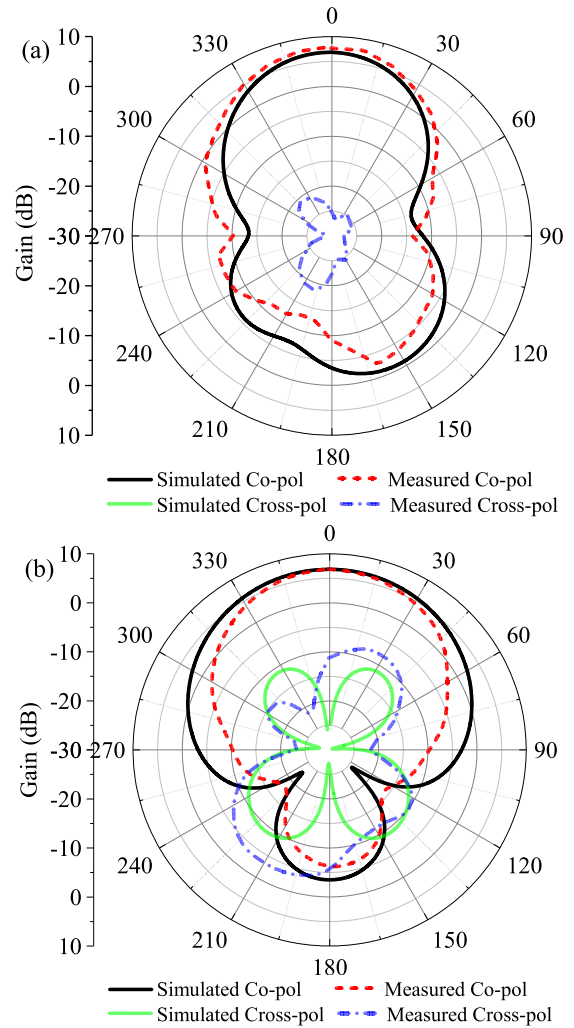


FIGURE 14. Gain patterns of LP mode at 45° azimuth on the (a) co-polar plane and (b) cross-polar plane.

azimuth of the linear polarization plane are $45^\circ, 60^\circ, 30^\circ, 90^\circ, 0^\circ, 120^\circ, 135^\circ$ and 150° , respectively. The surface electrical field distributions at different time in one sinusoidal period are plotted in Figs.10 (a)-(h), respectively. When the antenna works in any LP mode, the electrical field vectors are always point in one direction, meanwhile the amplitudes have maximum values at time $t = 0$ or $T/2$ and have minimum values at time $t = T/4$ or $3T/4$. The phase parameter α can be arbitrarily designated, thus the LP plane of the antenna can be continuously controlled within the total azimuth direction of 360° .

Finally, the radiation patterns of the antenna working in LHCP mode, RHCP mode and four LP modes with different polarization plane are simulated and measured, as shown in Figs.11-14, respectively.

When the antenna works in LHCP mode, the measured and simulated peak gain in the main radiation direction reaches about 6.8dBi, and the maximum cross-polarization gain level is below -7.2 dBi in xz -plane and -5.6 dBi

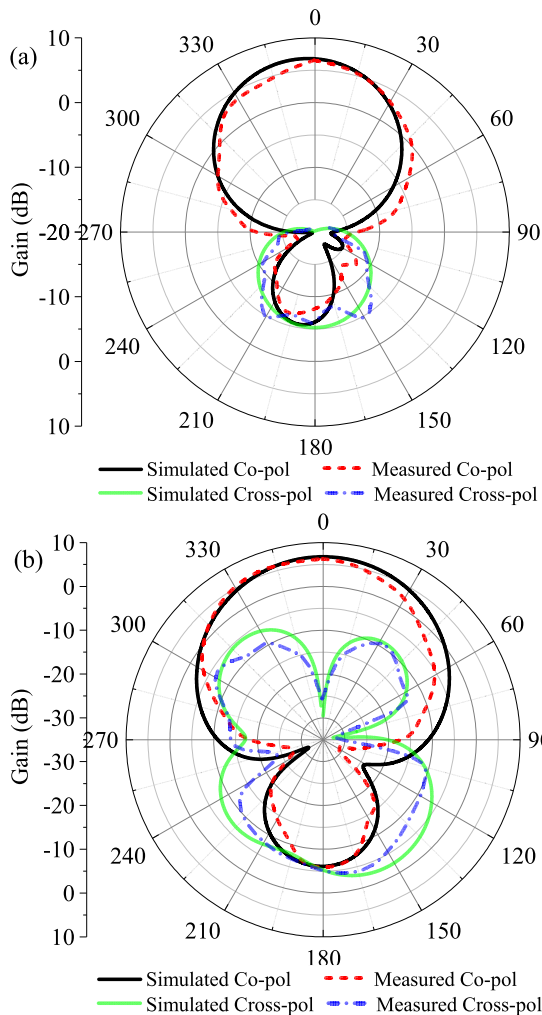


FIGURE 15. Gain patterns of LP mode at 90° azimuth on the (a) co-polar plane and (b) cross-polar plane.

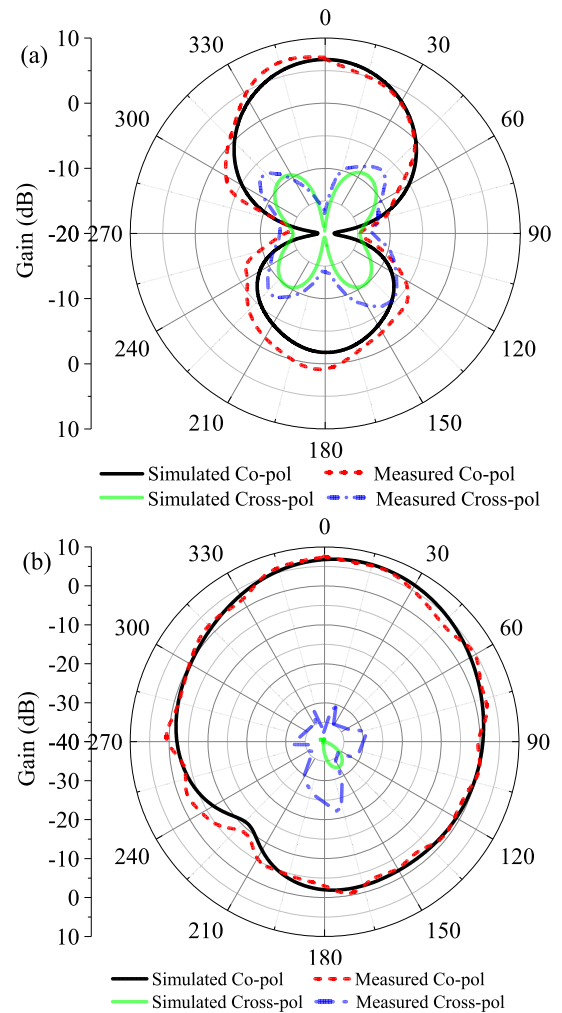


FIGURE 16. Gain patterns of LP mode at 135° azimuth on the (a) co-polar plane and (b) cross-polar plane.

in yz -plane, as shown in Figs.11 (a) and (b), respectively. When the antenna works in RHCP mode, the measured and simulated peak gain are both about 6.8dBi as well, and the simulated maximum cross-polarization gain level is below -5.6 dBi in xz -plane and -4.8 dBi in yz -plane, as shown in Figs.12 (a) and (b), respectively. As shown in Fig.13 (a) and (b), the peak gain remains at about 6.8 dBi when the antenna work in LP mode with polarization plane at azimuth of 0° , and the simulated maximum cross-polarization gain level is below -5.5 dBi in the co-polarization plane (xz -plane) and -4.9 dBi in cross-polarization plane (yz -plane), respectively. As the azimuth of polarization plane is adjusted to 45° , the peak gain remains about 6.8 dBi as well, and the measured maximum cross-polarization gain level is below -18.5 dBi in the co-polarization plane (plane oriented in azimuth of 45°) and -3.2 dBi in cross-polarization plane (plane oriented in azimuth of 135°), as shown in Fig.14 (a) and (b), respectively. It should be mentioned that the simulated cross-polarization gain level in co-polar plane is below -35 dBi, resulting in no appearance in Fig. 14(a).

Similarly, the gain patterns are simulated and measured when the antenna operates in LP modes with its polarization plane oriented in azimuth of 90° and 135° , as shown in Figs. 15 and 16, respectively. The cross-polarization gain levels still remain low values in both the co-polarization plane, as illustrated in Fig.15 (a) and Fig.16 (a), and cross-polarization plane, as depicted in Fig.15 (b) and Fig.16 (b). In addition, the gain difference between the co-polarization and cross-polarization components is beyond 40 dBi for all the polarization states in the main radiation direction, which indicates a high polarization purity of the proposed antenna. As shown in Figs. 12 to 16, the measured gain patterns agree well with the simulated ones, and the slight deviation is likely caused by the measurement and fabrication tolerances.

IV. CONCLUSION

In conclusion, a polarization-reconfigurable antenna is proposed based on the CP mode combination technique. The LHCP and RHCP modes can be independently generated with very low crosstalk when only one of the feeding

microstrip lines is excited. By simultaneously exciting the two feeding microstrip lines with identical amplitudes but a changeable initial phase difference through a feeding circuit, an LP wave can be obtained with its polarization plane at any desired azimuth angle, which means that the polarization plane can be continuously turned by properly tuning the initial phase difference between the two feeding ports of the antenna. To verify the design concept, a prototype has been fabricated and measured. The measured results are in good agreement with the simulated ones for all the polarization states. The proposed antenna can be used to transmit and receive CP waves and LP wave polarized at any azimuth, well avoiding the polarization mismatch.

REFERENCES

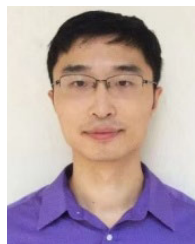
- [1] D. Piazza, N. J. Kirsch, A. Forenza, R. W. Heath, and K. R. Dandekar, "Design and evaluation of a reconfigurable antenna array for MIMO systems," *IEEE Trans. Antennas Propag.*, vol. 56, no. 3, pp. 869–881, Mar. 2008.
- [2] P.-Y. Qin, Y. J. Guo, and C.-H. Liang, "Effect of antenna polarization diversity on MIMO system capacity," *IEEE Antennas Wireless Propag. Lett.*, vol. 9, pp. 1092–1095, 2010.
- [3] D. Piazza, P. Mookiah, M. D'Amico, and K. R. Dandekar, "Experimental analysis of pattern and polarization reconfigurable circular patch antennas for MIMO systems," *IEEE Trans. Veh. Technol.*, vol. 59, no. 5, pp. 2352–2362, Jun. 2010.
- [4] M. A. Kossel, R. Kung, H. Benedickter, and W. Biichtokd, "An active tagging system using circular-polarization modulation," *IEEE Trans. Microw. Theory Techn.*, vol. 47, no. 12, pp. 2242–2248, Dec. 1999.
- [5] H. A. Zebker and J. J. Van Zyl, "Imaging radar polarimetry: A review," *Proc. IEEE*, vol. 79, no. 11, pp. 1583–1606, Nov. 1991.
- [6] E. Al Abbas, N. Nguyen-Trong, A. T. Mobashsher, and A. M. Abbosh, "Polarization-reconfigurable antenna array for millimeter-wave 5G," *IEEE Access*, vol. 7, pp. 131214–131220, 2019.
- [7] M.-C. Tang, Z. Wu, T. Shi, and R. W. Ziolkowski, "Electrically small, low-profile, planar, Huygens dipole antenna with quad-polarization diversity," *IEEE Trans. Antennas Propag.*, vol. 66, no. 12, pp. 6772–6780, Dec. 2018.
- [8] S.-L.-S. Yang and K.-M. Luk, "A wideband L-probes fed circularly-polarized reconfigurable microstrip patch antenna," *IEEE Trans. Antennas Propag.*, vol. 56, no. 2, pp. 581–584, Feb. 2008.
- [9] Y. Cao, S. W. Cheung, and T. I. Yuk, "A simple planar polarization reconfigurable monopole antenna for GNSS/PCS," *IEEE Trans. Antennas Propag.*, vol. 63, no. 2, pp. 500–507, Feb. 2015.
- [10] W. Lin and H. Wong, "Polarization reconfigurable aperture-fed patch antenna and array," *IEEE Access*, vol. 4, pp. 1510–1517, 2016.
- [11] M. N. Osman, M. K. A. Rahim, M. R. Hamid, M. F. M. Yusoff, and H. A. Majid, "Compact dual-port polarization-reconfigurable antenna with high isolations for MIMO application," *IEEE Antennas Wireless Propag. Lett.*, vol. 15, pp. 456–459, 2016.
- [12] H. Sun and S. Sun, "A novel reconfigurable feeding network for quad-polarization-agile antenna design," *IEEE Trans. Antennas Propag.*, vol. 64, no. 1, pp. 311–316, Jan. 2016.
- [13] L.-Y. Ji, P.-Y. Qin, Y. J. Guo, C. Ding, G. Fu, and S.-X. Gong, "A wide-band polarization reconfigurable antenna with partially reflective surface," *IEEE Trans. Antennas Propag.*, vol. 64, no. 10, pp. 4534–4538, Oct. 2016.
- [14] J. Hu, G. Q. Luo, and Z.-C. Hao, "A wideband quad-polarization reconfigurable metasurface antenna," *IEEE Access*, vol. 6, pp. 6130–6137, 2018.
- [15] R. Lian, Z. Tang, and Y. Yin, "Design of a broadband polarization-reconfigurable Fabry–Pérot resonator antenna," *IEEE Antennas Wireless Propag. Lett.*, vol. 17, no. 1, pp. 122–125, Jan. 2018.
- [16] P.-Y. Qin, A. R. Weily, Y. J. Guo, and C.-H. Liang, "Polarization reconfigurable U-slot patch antenna," *IEEE Trans. Antennas Propag.*, vol. 58, no. 10, pp. 3383–3388, Oct. 2010.
- [17] M. S. Nishamol, V. P. Sarin, D. Tony, C. K. Aanandan, P. Mohanan, and K. Vasudevan, "An electrically reconfigurable microstrip antenna with switchable slots for polarization diversity," *IEEE Trans. Antennas Propag.*, vol. 59, no. 9, pp. 3424–3427, Sep. 2011.
- [18] X.-X. Yang, B.-C. Shao, F. Yang, A. Z. Elsherbeni, and B. Gong, "A polarization reconfigurable patch antenna with loop slots on the ground plane," *IEEE Antennas Wireless Propag. Lett.*, vol. 11, pp. 69–72, 2012.
- [19] A. Khidre, K.-F. Lee, F. Yang, and A. Z. Elsherbeni, "Circular polarization reconfigurable wideband E-shaped patch antenna for wireless applications," *IEEE Trans. Antennas Propag.*, vol. 61, no. 2, pp. 960–964, Feb. 2013.
- [20] S. W. Lee and Y. J. Sung, "Simple polarization-reconfigurable antenna with T-shaped feed," *IEEE Antennas Wireless Propag. Lett.*, vol. 15, pp. 114–117, 2016.
- [21] P. Kumar, S. Dwari, R. K. Saini, and M. K. Mandal, "Dual-band dual-sense polarization reconfigurable circularly polarized antenna," *IEEE Antennas Wireless Propag. Lett.*, vol. 18, no. 1, pp. 64–68, Jan. 2019.
- [22] W.-S. Yoon, J.-W. Baik, H.-S. Lee, S. Pyo, S.-M. Han, and Y.-S. Kim, "A reconfigurable circularly polarized microstrip antenna with a slotted ground plane," *IEEE Antennas Wireless Propag. Lett.*, vol. 9, pp. 1161–1164, 2010.
- [23] X.-T. Yang, H. Wong, and J. Xiang, "Polarization reconfigurable planar inverted-F antenna for implantable telemetry applications," *IEEE Access*, vol. 7, pp. 141900–141909, 2019.
- [24] E. Cil and S. Dumanli, "The design of a reconfigurable slot antenna printed on glass for wearable applications," *IEEE Access*, vol. 8, pp. 95417–95423, 2020.
- [25] C. Ni, M. S. Chen, Z. X. Zhang, and X. L. Wu, "Design of frequency- and polarization-reconfigurable antenna based on the polarization conversion metasurface," *IEEE Antennas Wireless Propag. Lett.*, vol. 17, no. 1, pp. 78–81, Jan. 2018.
- [26] W. Li, S. Gao, Y. Cai, Q. Luo, M. Sobhy, G. Wei, J. Xu, J. Li, C. Wu, and Z. Cheng, "Polarization-reconfigurable circularly polarized planar antenna using switchable polarizer," *IEEE Trans. Antennas Propag.*, vol. 65, no. 9, pp. 4470–4477, Sep. 2017.
- [27] H. H. Tran, N. Nguyen-Trong, T. T. Le, A. M. Abbosh, and H. C. Park, "Low-profile wideband high-gain reconfigurable antenna with quad-polarization diversity," *IEEE Trans. Antennas Propag.*, vol. 66, no. 7, pp. 3741–3746, Jul. 2018.
- [28] S.-L. Chen, F. Wei, P.-Y. Qin, Y. J. Guo, and X. Chen, "A multi-linear polarization reconfigurable unidirectional patch antenna," *IEEE Trans. Antennas Propag.*, vol. 65, no. 8, pp. 4299–4304, Aug. 2017.
- [29] C. Xu, Y. Wang, J. Wu, and Z. Wang, "Parasitic circular patch antenna with continuously tunable linear polarization using liquid metal alloy," *Microw. Opt. Technol. Lett.*, vol. 61, no. 3, pp. 727–733, Mar. 2019.
- [30] C. Xu, Z. Wang, Y. Wang, P. Wang, and S. Gao, "A polarization-reconfigurable wideband high-gain antenna using liquid metal tuning," *IEEE Trans. Antennas Propag.*, vol. 68, no. 8, pp. 5835–5841, Aug. 2020.
- [31] F. Ferrero, C. Luxey, R. Staraj, G. Jacquemod, M. Yedlin, and V. F. Fusco, "Patch antenna with linear polarization tilt control," *Electron. Lett.*, vol. 45, no. 17, pp. 870–872, Aug. 2009.
- [32] M. Sano and M. Higaki, "A linearly polarized patch antenna with a continuously reconfigurable polarization plane," *IEEE Trans. Antennas Propag.*, vol. 67, no. 8, pp. 5678–5683, Aug. 2019.
- [33] K. Li, Y. Shi, H. Shen, and L. Li, "A characteristic-mode-based polarization-reconfigurable antenna and its array," *IEEE Access*, vol. 6, pp. 64587–64595, 2018.



SHENYUN WANG (Member, IEEE) was born in Hubei, China, in 1981. He received the Ph.D. degree in information and communication system from the Nanjing University of Aeronautics and Astronautics, Nanjing, China, in 2012. From 2009 to 2011, he was a Visiting Ph.D. Student with the National University of Singapore, Singapore. He currently works as an Associate Professor with the School of Electronic and Information Engineering, Nanjing University of Information Science and Technology, Nanjing. His current research interests include the microwave theory and technology, reconfigurable antennas, array antennas, and electromagnetic compatibility.



DANPING YANG was born in Anhui, China, in 1995. She is currently pursuing the M. Eng. degree in electrical engineering with the Nanjing University of Information Science and Technology, Jiangsu, China. Her research interests include RF circuit and reconfigurable antenna.



CHEN ZHAO (Member, IEEE) received the B.Eng. degree from the University of Electronic Science and Technology of China, Chengdu, China, in 2011, and the Ph.D. degree from Nanyang Technological University, Singapore, in 2016. From 2015 to 2017, he was a Research Scientist with Temasek Laboratories, National University of Singapore, Singapore. He is currently with the Nanjing University of Information Science and Technology, Nanjing, China. His current research interests include characteristic mode for antenna design, functional metamaterial, and millimeter-wave vacuum electronic devices.



WEN GEYI (Fellow, IEEE) was born in Pingjiang, Hunan, China, in 1963. He received the B. Eng., M. Eng., and Ph. D. degrees in electrical engineering from Xidian University, Xi'an, China, in 1982, 1984, and 1987, respectively. From 1988 to 1990, he was a Lecturer with the Radio Engineering Department, Southeast University, Nanjing, China. From 1990 to 1992, he was an Associate Professor with the Institute of Applied Physics, University of Electronic Science and Technology of China (UESTC), Chengdu, China. From 1992 to 1993, he was a Visiting Researcher with the Department of Electrical and Computer Engineering, University of California at Berkeley, Berkeley, CA, USA. From 1993 to 1998, he was a Full Professor with the Institute of Applied Physics, UESTC. He was a Visiting Professor with the Electrical Engineering Department, University of Waterloo, Waterloo, ON, Canada, from February 1998 to May 1998. From 1996 to 1997, he was the Vice Chairman of the Institute of Applied Physics, UESTC, where he was the Chairman of the Institute, from 1997 to 1998. From 1998 to 2007, he was with Blackberry Ltd., Waterloo, first as a Senior Scientist with the Radio Frequency Department, and then the Director of the Advanced Technology Department. Since 2010, he has been a National Distinguished Professor with Fudan University, Shanghai, China, and the Nanjing University of Information Science and Technology (NUIST), Nanjing. He is currently the Director of the Research Center of Applied Electromagnetics, NUIST. He has authored over 100 publications and Foundations for Radio Frequency Engineering (World Scientific, 2015), the Foundations of Applied Electrodynamics (Wiley, 2010), Advanced Electromagnetic Field Theory (China: National Defense Publishing House, 1999), and the Modern Methods for Electromagnetic Computations (China: Henan Science and Technology Press, 1994). He holds more than 40 patents. His current research interests include microwave theory and techniques, and antennas and wave propagation.



GUOWEN DING (Member, IEEE) received the B.S. degree in electronic information science and engineering and the M.S. degree in electronic and communication engineering from the Nanjing University of Aeronautics and Astronautics, Nanjing, China, in 2013 and 2016, respectively, and the Ph.D. degree in electronic science and engineering from Nanjing University, Nanjing, in 2020. He is currently with the School of Electronic and Information Engineering, Nanjing University of Information Science and Technology, Nanjing. His research interests include microwave theory and technology, antenna, electromagnetic metamaterials, and metasurface.

• • •